Express Polymer Letters Vol.17, No.10 (2023) 1042–1055
Available online at www.expresspolymlett.com
https://doi.org/10.3144/expresspolymlett.2023.78

Research article

Synthesis and evaluation of poly(isoprene-*co*-acrylonitrile) as synthetic rubber with enhanced oil resistance

*Zhen Hern Boon, Yin Yin Teo, Desmond Teck-Chye Ang**

Department of Chemistry, Universiti Malaya, 50603 Kuala Lumpur, Malaysia

Received 20 March 2023; accepted in revised form 11 July 2023

Abstract. Increasing demand for durable rubber and rapid advancement in the automotive sector has made oil-resistant rubber an increasingly important material. Among them, nitrile rubber (NBR) is the most iconic due to its extraordinary oil resistance contributed by the polar nitrile pendant groups. Synthesis of NBR, however, is highly hazardous due to the explosive nature of the gaseous monomer butadiene. In this work, poly(isoprene-*co*-acrylonitrile) (NIR) was synthesized using free radical emulsion polymerization, with liquid monomer isoprene as the diene in the rubber formulation. The spectroscopic analysis confirmed the formation of NIR and indicated that the polymerized isoprene in the rubber is predominantly of 1,4-microstructure. A series of rubbers with different contents of acrylonitrile were produced and the mechanical, thermal, as well as oil resistant property of the resultant rubber films were evaluated. Vulcanized NIR films displayed glass transition temperatures from –9.4 to 20.2 °C, suggesting that the polymers are rubbery at ambient and higher temperatures. The NIR rubber films exhibited excellent oil resistance with less than 2% swelling in mineral oil, good thermal stability with onset degradation temperature in the range of 361.3 to 369.9 °C, and adequate mechanical strength from 1.61 to 8.23 MPa. The synthesized NIR rubber has the potential to serve as an alternative to NBR which had been traditionally used for oil resistance applications.

Keywords: *elastomer, synthetic rubber, thermal degradation, radical polymerization, tensile testing, oil resistance*

1. Introduction

Rubbers are generally amorphous polymeric materials categorized as elastomers [1]. Depending on the origin, rubbers can be divided into natural rubber (NR) and synthetic rubber. NR is obtained from the coagulation of latex in rubber trees, and *Hevea brasiliensis* is the current dominant species for natural rubber production [2, 3], while synthetic rubber refers to those which were synthesized from monomers. Although the monomers used in rubber synthesis were mostly petroleum-derived, there are, however increasing number of initiatives to produce bio-based synthetic rubbers utilizing materials that were sourced naturally [4, 5]. According to a report by the International Rubber Study Group, the world consumption of natural and synthetic rubbers in the year 2021 was reported at 13.77 million metric tons and 15.81 million metric tons, respectively. The consumption of both rubbers is forecasted to increase by 2.8 and 2.9%, respectively, in the year 2023, and the total rubber demand is expected to grow on an average of 2.4% per annum until the year 2031. The high volume of rubber consumption is a result of a wide range of applications of rubber in various fields.

Although NR is irreplaceable in terms of mechanical strength due to its exceptionally high molecular weight, good fatigue resistance and ability to undergo stress crystallization [3, 6, 7], NR's lack of resistance to strong sunlight, oxidative and oily environment, as well as inconsistent supply of global NR stock had made the shift to synthetic rubber inevitable [2, 3, 8, 9]. Synthetic rubbers provide an extended

*Corresponding author, e-mail: desmond860108@um.edu.my

range of applications on top of the applications of NR. The chemical structure of synthetic rubber can be varied using different amounts and combinations of monomers, resulting in rubbers with a vast range of properties. For example, nitrile-butadiene rubber (NBR), more commonly called nitrile rubber, is obtained through emulsion polymerization of butadiene and acrylonitrile. The most significant characteristic of NBR is its excellent oil resistance contributed by the polar nitrile group [10]. Commonly, the acrylonitrile content (ACN content) in NBR ranges from 18 to 50%, and the oil resistance property improves with the increase in ACN content [3, 10]. ACN content in NBR can also be used to tailor other properties such as mechanical properties, glass transition temperature, T_g, and processability of the rubber [3]. The presence of polar nitrile groups resists the penetration of non-polar oils into the rubber structure, resulting in lesser swelling, and allows the rubber to retain its original properties and dimensions when in contact with oil. This makes nitrile rubber an excellent material for applications such as O-rings, gaskets, and hoses in the automotive, aeronautical, oil and gas industry [11]. Besides oil-sealing purposes, NBR was also exploited to produce nitrile gloves, especially after increased public awareness about latex protein allergy from natural rubber latex gloves. Wider chemical resistance coverage, higher puncture resistance, and aging resistance are some of the additional features that make nitrile disposable gloves preferred in the medical sector, laboratories, and food industries [11, 12].

Whilst NBR is an important synthetic rubber, production of the rubber could be a highly challenging ordeal. Butadiene or 1,3-butadiene is a 4-carbon conjugated diene that is used in the synthesis of nitrile rubber. It is a colorless gas that is commercially produced through steam cracking of crude oil [13]. In addition to the extra setups necessary to operate a gaseous monomer, the production of NBR is relatively risky due to the flammability and explosive nature of butadiene when mixed with air. Incidents of fire and explosion at processing facilities related to butadiene could happen even with slight negligence. There were several reported cases in recent years, such as a chemical plant explosion in Port Neches, Texas, on November 2019, an explosion and fire at an emulsion styrene-butadiene rubber production plant in Poland on January 2021, and a major fire at a butadiene rubber plant in Malaysia on February 2022. It is therefore necessary to explore alternative diene, which is easier and less risky to operate for the production of synthetic rubber with properties similar to that of NBR, specifically its superior oil resistance.

Isoprene or 2-methyl-1,3-butadiene, is a 5-carbon conjugated diene that is widely used in the rubber industry. Isoprene is the main constituent of NR and synthetic polyisoprene (PIP). It is also used in other synthetic rubbers, such as butyl rubber (IIR) and styrene-isoprene block copolymers (SIS) [3]. Isoprene can be polymerized through various techniques, including anionic, cationic, free radical and coordination polymerizations. The coordination polymerization using Ziegler-Natta catalysts is preferred in the industrial synthesis of PIP due to the ability to produce high *cis*-1,4-polyisoprene content, enabling the rubber to exhibit properties similar to NR [3, 14]. The polymerization of isoprene is often investigated and compared alongside butadiene. This is because they are considered close analogous conjugated dienes due to their similarity in chemical structure, oftentimes resulting in similar polymerization kinetics [15, 16]. Some recent research on the polymerization of isoprene is focused on the emulsion polymerization with the objectives of improving the polymerization rate and yield, as conventional emulsion polymerization of isoprene had low yield due to low propagation rate, high termination, and side reactions [16, 17]. Different initiator systems in the emulsion polymerization of PIP were investigated by Cheong *et al.* [18] in 2004. They found the redox initiator systems allowed the low-temperature polymerization temperature at 25 °C, resulting in higher yield polymerization and produced PIP with negligible gel content. Chouytan *et al.* [19] reported the improvement in monomer conversion in miniemulsion polymerization of isoprene by controlling the ratio of surfactant-to-monomer concentration, causing an increase in number of stabilized emulsion droplets and thus the loci for polymerization reaction.

In view of the need to overcome the limitation of butadiene in nitrile rubber formulation and the lack of potential alternatives to NBR, this work details the development of poly(isoprene-*co*-acrylonitrile), NIR as a new synthetic rubber with excellent oil resistance. No gaseous monomers were used in the synthesis, and isoprene, which is a liquid diene monomer at ambient temperature, was used to produce the rubber emulsion in a simple one-pot synthesis setup.

The nitrile content of the rubber varied from 20 to 35 mol%, and the resultant properties of the emulsion and rubber films were evaluated. The chemical structure of the rubber was characterized using Fourier transform infrared spectroscopy (FTIR) and proton nuclear magnetic resonance (^{1}H-NMR), while mechanical properties and oil resistance tests were conducted on the vulcanized rubber films.

2. Experimental

2.1. Materials

Synthesis grade isoprene (CAS: 78-79-5) and acrylonitrile (CAS: 107-13-1) were obtained from Merck (Germany). Analysis grade potassium peroxodisulfate ($K_2S_2O_8$, CAS: 7727-21-1), sodium dithionite ($Na_2S_2O_4$, CAS: 7775-14-6), sodium hydroxide (NaOH) pellets (CAS: 1310-73-2) and 28–30% ammonia solution (CAS: 1336-21-6) were obtained from Merck (Germany). Isooctyl 3-mercaptopropionate (≥99%, CAS: 30374-02-7), technical grade sodium dodecylbenzenesulfonate (SDBS, CAS: 25155-30-0) and chloroform-D ($CDCl_3$) (99.8 atom% D, contains 0.03 v/v% tetramethylsilane (TMS), CAS: 865-49-6) were obtained from Sigma Aldrich (Germany). Total Quartz 5000 Future 10W-30 mineral-based engine oil was obtained from Total Oil Asia-Pacific Pte Ltd, Singapore. 50 wt% zinc dithiocarbamates (ZDBC) dispersion, 60 wt% zinc oxide (ZnO) dispersion, and 60 wt% sulphur dispersion were obtained from Aquaspersions (M) Sdn Bhd. NBR latex was purchased from Crucial (M) Sdn. Bhd. The properties of NBR used is given in Table 1. All chemicals involved in this work were used as received except for isoprene and acrylonitrile, which both were washed with 10 wt% NaOH solution and distilled water to remove inhibitors prior to usage.

2.2. Synthesis of poly(isoprene-*co*-acrylonitrile) emulsion

A series of poly(isoprene-*co*-acrylonitrile) (NIR) rubber varying in ACN content were synthesized through emulsion polymerization, and the formulations are given in Table 2. The methodology of emulsion polymerization for NIR rubber was adapted from [20, 21]. Codename NIR20 was given to NIR with 20 mol% ACN content, and the same codename format is applicable for NIR30 and NIR35. The highest ACN content in this work was fixed at 35%, as excessively high nitrile content in NIR leads to stiffer material with reduced elasticity. The polymerization was carried out at 65–70 °C in a 2 l reaction flask while being constantly stirred at 60–80 rpm with an overhead stirrer. A double condenser system attached to cold water supply was used to increase the condensation efficiency of low boiling point isoprene and enable the collection of condensates at the end of the second condenser, which was then reintroduced back into the reaction flask throughout the synthesis. The reaction setup is shown in Figure 1. SDBS was dissolved in distilled water bubbled with nitrogen gas, adjusted to pH 7–9 with ammonia solution, and then transferred to the reaction flask. The initiator, $K_2S_2O_8$, was dissolved in 200 ml of distilled water, while the activator, $Na_2S_2O_4$, was dissolved in 100 ml of distilled water. The initiator and activator solution were premixed and the mixture was then added dropwise into the flask over a period of 12 h, while the monomers mixture was added dropwise concurrently over the first 8 h. Chain transfer agent (CTA) isooctyl 3-mercaptopropionate was added into the mixture starting from the second half of the monomer addition. At the end of the synthesis, the pH of the mixtures was adjusted to pH 9–10 to preserve the stability of the emulsion.

Table 1. Properties of NBR.

Property		Quantity
Total solid content, *TSC*	[%]	45
Nitrile content	[%]	<30
Molecular weight	[·10^5 kDa]	1.45
Viscosity at 25±2 °C	[mPa·s]	38
pH		8.2

2.3. Characterization of rubber emulsions

The total solid content (*TSC*) of the rubber emulsions was measured according to ASTM D1417. A clean, dry aluminum foil dish was weighed (m_1), and approximately 2 ml of rubber emulsion was transferred

Table 2. NIR rubber formulations.

Ingredient	Formulation [g]		
	NIR20	NIR30	NIR35
Isoprene	272.500	238.400	221.400
Acrylonitrile	53.060	79.590	92.860
$K_2S_2O_8$	4.866	4.866	4.866
$Na_2S_2O_4$	3.134	3.134	3.134
CTA	4.883	4.770	4.714
SDBS	17.360	17.000	16.820
Water	308.700	296.700	290.700

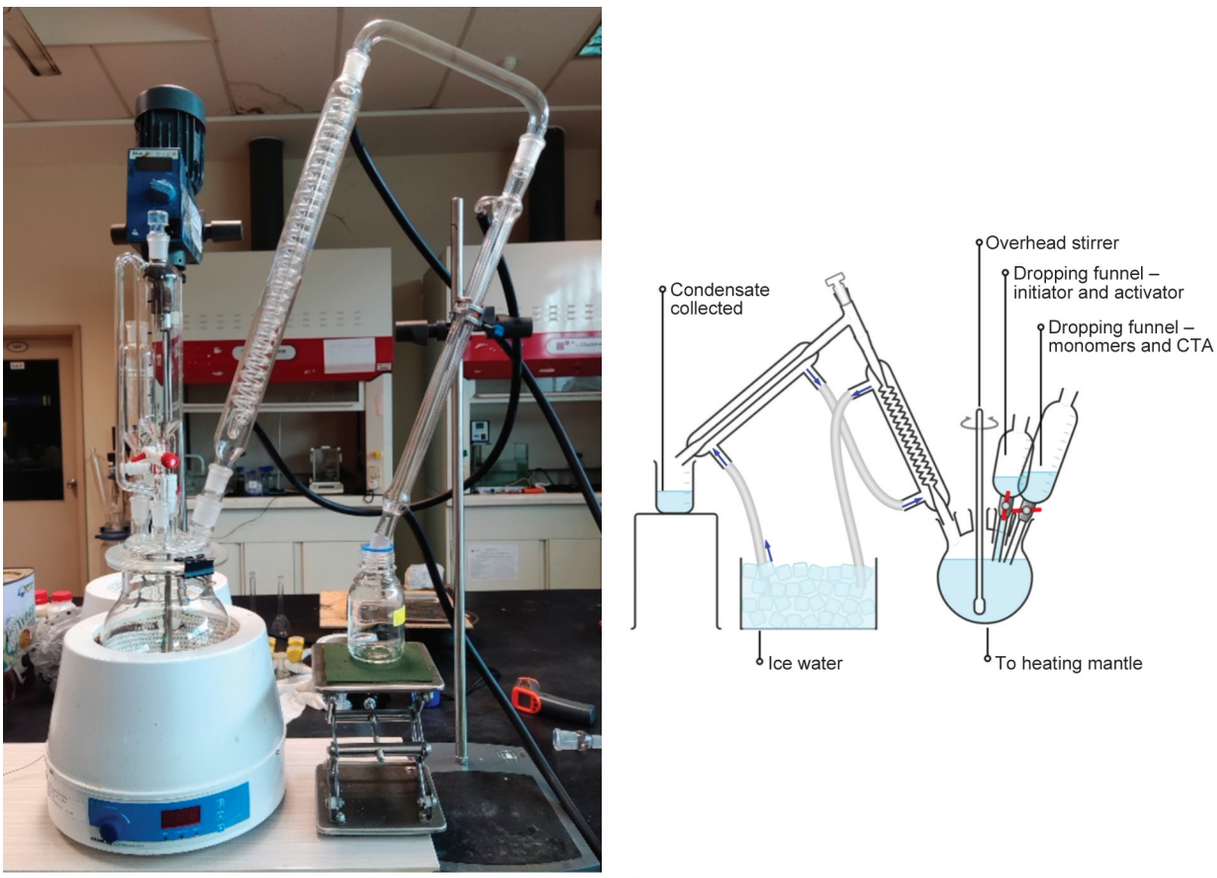

Figure 1. Apparatus setup for emulsion polymerization of NIR a) actual setup, and b) schematic diagram.

to the aluminum foil dish with a dropper and weighed (m_2). The aluminum foil dish with rubber emulsion was then heated in an oven at 170 °C for 15 min before it was removed and cooled in a desiccator. After reaching room temperature, the aluminum foil dish was weighed (m_3). *TSC* was calculated according to Equation (1):

$$TSC\,[\%] = \frac{m_3 - m_1}{m_2 - m_1} \cdot 100 \tag{1}$$

The particle size (Z-average diameter) and zeta potential of the emulsions were measured using Malvern Zetasizer NanoZS at 25 °C. Folded capillary cells D*TS*1070 were used in both measurements. The emulsion was first diluted with distilled water before analysis to weaken the scattering signal and improve the accuracy of the analysis. The viscosity of the rubber emulsions was measured using NDJ-1 digital rotary viscometer. The solid content of all emulsions was adjusted and standardized to 30 w/w% before measurement, and Rotor #1 at a spindle velocity of 60 rpm was used. The viscosity reported was from the average of 3 readings. Molecular weight measurement was carried out utilizing the static light scattering technique. A series of rubber emulsions with different concentrations were prepared through dilution with distilled water. The scattering intensities were measured using Malvern Zetasizer NanoZS at a wavelength of 632.8 nm, scattering detection angle of 173°, and temperature of 25 °C. Distilled water was used as the scattering standard and the refractive index increment (d_n/d_c) was 0.118. The molecular weight was determined from the Debye plot.

2.4. Compounding and preparation of NIR film

Compounding of the rubber emulsions was done through the addition of 2 parts per hundred parts dried rubber [phr] ZnO, 1 phr ZDBC, 1 phr sulphur and 0.5 phr ammonia solution per 100 phr NIR rubber. The mixture was stirred at high-speed using an overhead stirrer overnight, and the mixture was left for another day for maturation. The pH of the mixture was adjusted to 9–10 after compounding. Rubber film was prepared through solution casting in Petri dishes. The amount of emulsion introduced into each petri dish was calculated based on the *TSC* of the rubber emulsion. It is necessary to ensure that a comparable

amount of rubber in each dish so that uniform and comparable film thickness can be obtained across different casted films. The Petri dishes were then dried in the fume hood overnight, followed by thorough drying in a thermal oven at 120 °C. The same formulation and compounding procedure was used to prepare NBR film for comparison purposes.

2.5. Characterization of rubber film

2.5.1. Spectroscopic characterization

Fourier transform infrared (FTIR) spectra of the rubber films were recorded using Attenuated Total Reflectance (ATR)-Perkin Elmer Frontier FTIR spectrometer in the region 550 to 4000 cm^{-1} at the resolution of 4 cm^{-1}. The spectrum recorded was from an average of 16 scans. The ^{1}H-NMR spectra of rubber films dissolved in $CDCl_3$ were recorded using JEOL ECX-400 FT-NMR spectrometer with traces of TMS present in the deuterated solvent to produce an internal reference signal at 0 ppm. It is noteworthy that spectroscopic analyses were conducted on uncompounded rubber films to avoid interference from the compounding ingredients.

2.5.2. Thermal analysis

Calorimetric analysis was done using the TA Instruments DSC Q20 differential scanning calorimeter (DSC) to determine the T_g of the rubber films. The temperature scan rate was 10 °C/min in the temperature range from –40 to 100 °C, and the nitrogen gas flow rate was at 200 ml/min. Thermogravimetric analysis (TGA) of the rubber films was carried out using Perkin Elmer TGA4000 with the temperature scan rate 10 °C/min in the temperature range from 30 to 900 °C.

2.5.3. Mechanical testing

A tensile test was carried out according to ASTM D412. Dumbbell-shaped rubber film with narrow section having 4 mm width, 10 mm length, and 1 mm thick were cut from the casted rubber films. The instrument used for the test was Shimadzu AG-5kNX Universal Tester with a crosshead speed of 500 mm/min. A tear strength test was carried out according to ASTM D624. Unnicked 90° sample was stretched using the same instrument and crosshead speed as the tensile test mentioned above. Ultimate tensile strength (*TS*), elongation at break (*EB*), modulus at 100% strain (*M100*), and tear strength (T_s) were determined and reported from the average of 3 repetitions.

2.5.4. Oil resistance test

The oil resistance test of the rubber films was carried out according to ASTM D471. Total Quartz 5000 Future 10W-30, a commonly used mineral-based engine oil, was used to test the oil resistance of the rubber. NR film was included in this test together with NIR and NBR samples for comparison purposes. Rectangular samples having a dimension of 25 mm width, 50 mm length, and 0.3 mm thickness were weighed (m_4) and hung on a self-made hanger using aluminum wire. The cut rubber samples were immersed in 100 cm^3 of testing oil for 72 h in the dark at room temperature (26±2 °C), 70±2 and at 100±2 °C. After the immersion period, the samples immersed at elevated temperature were cooled down to room temperature by transferring them into cool clean portion of the engine oil for 30–60 min. The samples were then dipped quickly in acetone and blotted lightly with lint-free filter paper before being weighed (m_5). The change in the mass of the sample was used to calculate the percentage swelling, which reflects the oil resistance of the rubber (Equation (2)):

$$\text{Percentage swelling}\,[\%] = \frac{m_5 - m_4}{m_4} \cdot 100 \qquad (2)$$

The changes in the dimension (length, width, and thickness) of the rubber films from the oil immersion were measured as well. The changes in dimension and percentage swelling were calculated individually, and a repetition of 3 samples was carried out for each type of rubber.

3. Result and discussion

3.1. Characterization of rubber emulsions

The visual appearance of NIR emulsions and NBR commercial latex is shown in Figures 2a and 2b. They were milky white with no noticeable visual difference between all emulsions. The physical appearance of all the rubber films, as shown in Figure 2c, was similar too, where they are all yellowish white in color. The stability of the emulsions was investigated using particle size and zeta potential analyses, and the result is tabulated in Table 3, while the particle size distribution curve of all the rubber emulsions is shown in Figure 3. All the NIR emulsions recorded small particle sizes, in the range of 90–122 nm, comparable

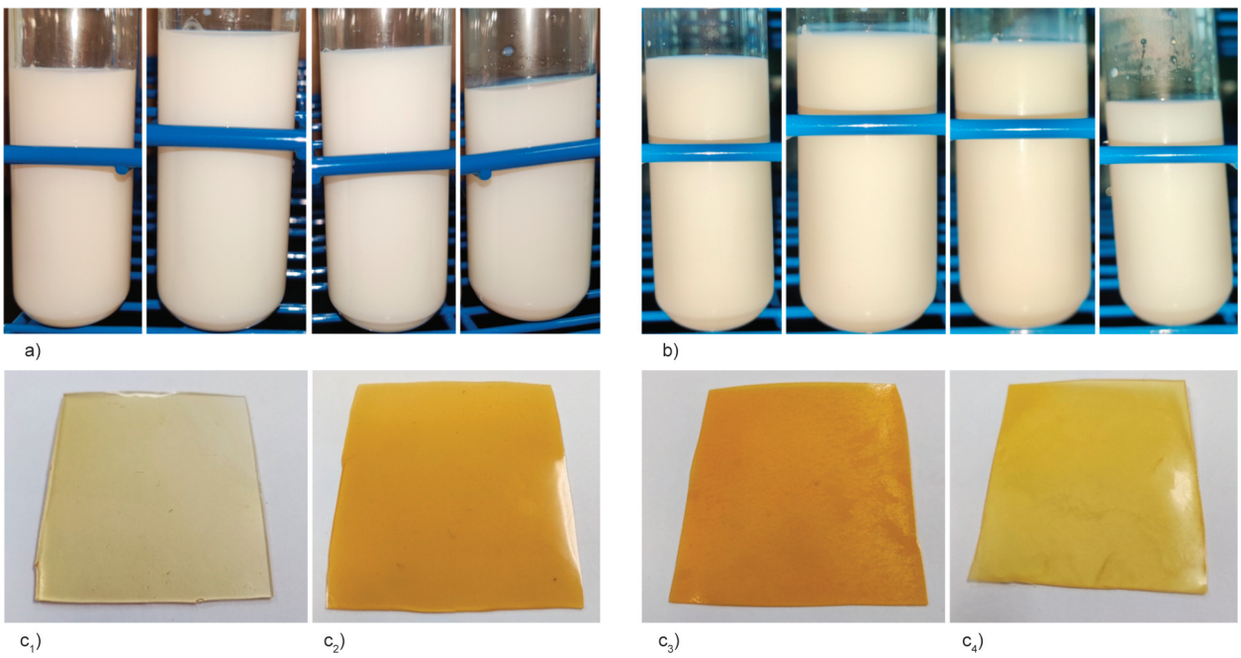

Figure 2. Physical appearance of rubber emulsions a) at freshly prepared, b) after 6 months storage (from left to right: NBR, NIR20, NIR30, NIR35), and c) vulcanized rubber films (c_1) NBR, c_2) NIR20, c_3) NIR30, c_4) NIR35).

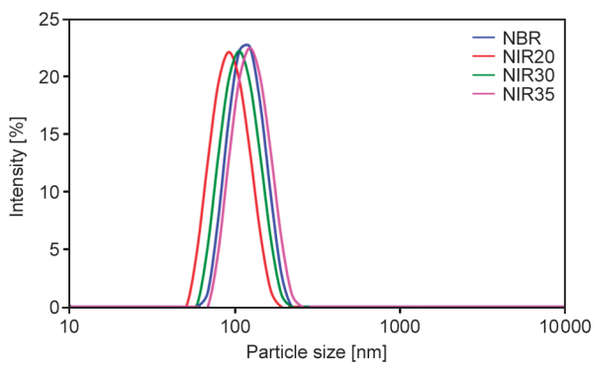

Figure 3. Particle size distribution curves of rubber emulsions.

to that of commercial NBR at 114 nm. Emulsion with smaller dispersed particle sizes was reported to be more stable as more particles can be distributed on the interface of the emulsion [22, 23]. All the NIR emulsions particles were also found to be narrowly distributed in size (monodisperse), which was evidenced by the low polydispersity index of less than 0.07 [24]. The Zeta potential of an emulsion can also be used to evaluate the stability of an emulsion, with those recording potential greater than |30 mV| usually considered sufficiently stable due to the strong electrostatic repulsion between the particles [25, 26]. NIR20 and NIR30 recorded high negative zeta potential exceeding –60 mV, while NIR35 had comparable zeta potential as the NBR at about –50 mV. The results imply that the synthesized emulsions were strongly anionic in nature and stable enough for long-term storage. The stability of the emulsions is also evidenced by the unnoticeable change in appearance after 6 months of storage, as shown in Figure 2b. The *TSC* of the NIR lattices produced was slightly less than 30%, and the concentration of all the lattices was adjusted to a uniform concentration of 30% *TSC* prior to viscosity measurement and film casting. It is noteworthy that the concentration of latex can be adjusted, for example, by removing water from the system or via centrifugation to obtain the desired concentration to suit the types of subsequent fabrication processes such as coagulant dipping, film casting, *etc*. The viscosity of all the emulsions was comparable at 5.6±0.2 mPa·s, suggesting that the molecular weight of the rubber in the emulsions may not differ significantly [27]. The molecular weight of

Table 3. Properties of NIR and NBR rubber emulsions.

Sample	Particle size [nm]	Polydispersity index	Zeta potential [mV]	Viscosity [mPa·s]	Molecular weight [·10^5 kDa]
NIR20	90.7	0.039	–63.3	5.44	3.44
NIR30	104.2	0.045	–61.0	5.44	1.53
NIR35	122.0	0.069	–50.1	5.58	0.91
NBR	113.7	0.044	–51.8	5.81	1.45

the rubber obtained from the light scattering analysis was recorded in Table 3, and NIR30 had the closest molecular weight to the commercial NBR.

3.2. Characterization of rubber films

3.2.1. Spectroscopic analysis

The FTIR spectrum of all samples is represented in Figure 4. The band at 1378 cm^{-1} represents the $–CH_3$ bending from the *cis*-1,4-polyisoprene unit, while bands that represent other microstructures, such as 890 cm^{-1} from $=CH_2$ bending of 3,4-unit and 911 cm^{-1} from $=CH_2$ bending of 1,2-unit are either very weak or not observed at all [28, 29]. It was reported that isoprene may undergo polymerization to produce 4 isomers, namely the 3,4-addition polymer, 1,2-addition polymer, *cis*-1,4 and *trans*-1,4 polyisoprene [3]. The structures of all 4 isomers are given in Figure 5. Considering that the bands of other isomers are not apparent, it could be implied that the NIR rubbers are made of predominantly 1,4 units, consistent with the results reported by others on emulsion polymerization of isoprene [17]. The band at 2250 cm^{-1} was assigned to the stretching of the nitrile group (–CN), and the intense band at 1440 cm^{-1} was assigned to the bending vibration of the methylene group ($–CH_2–$). The ratio of these two bands

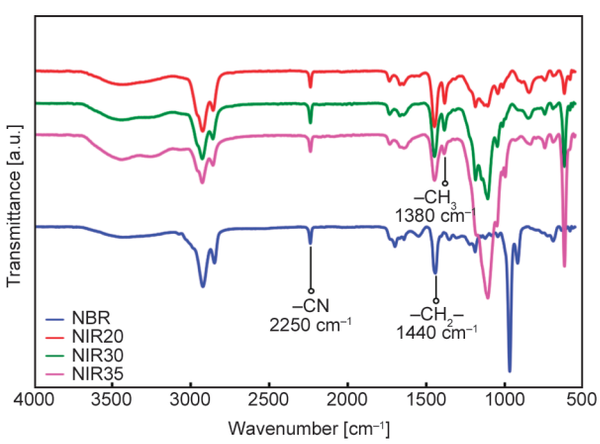

Figure 4. FTIR spectrum of NIR and NBR films.

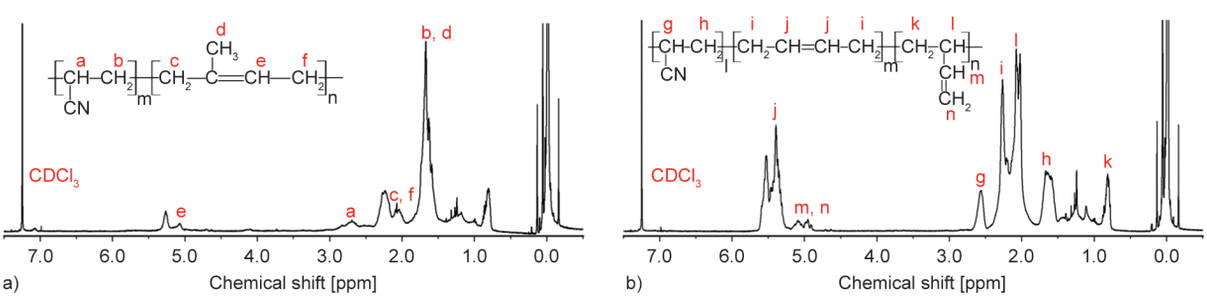

Figure 6. ^{1}H-NMR spectra of a) NIR30 and b) NBR.

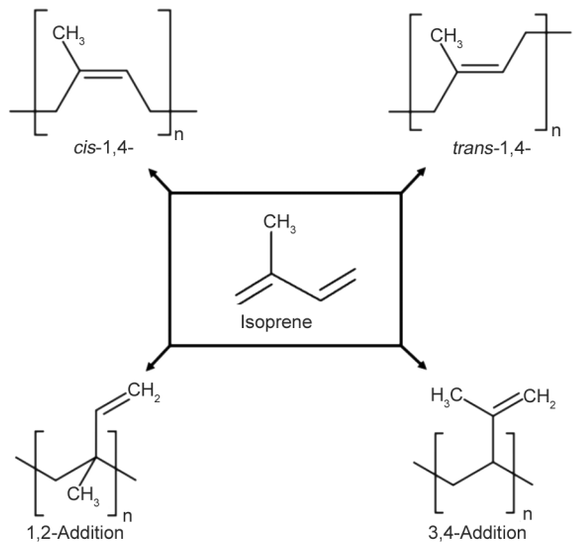

Figure 5. Chemical structure of isoprene and the respective polymerization isomers.

area, A_{2250}/A_{1440} reflects the relative amount of nitrile group present in the rubber, and values are tabulated in Table 4. The A_{2250}/A_{1440} value increased in the order of NIR20, NIR30 to NIR35, and this was well within expectation and consistent with the ACN content in the NIR rubber formulation (Table 2). The band area ratio for the NBR sample was close to those of NIR20 and NIR30, agreeing with the low nitrile grade of the NBR (Table 1).

Figure 6a shows the ^{1}H-NMR spectrum of NIR30. The chemical shift assignments are ($CDCl_3$; δ, ppm), 5.07 (=CH–, 1,4 unit) and 2.69 (CHCN, ACN). Other peaks at 2.07 and 1.67 ppm are from the resonance of protons attached to various groups, as labeled in the

Table 4. FTIR absorbance band area.

Sample	Band area		
	A_{2250}	A_{1440}	A_{2250}/A_{1440}
NIR20	64.47	499.4	0.129
NIR30	78.04	531.1	0.147
NIR35	138.70	574.2	0.242
NBR	85.55	549.1	0.156

figure. Consistent with the FTIR analysis, ^{1}H-NMR spectra of the NIR rubbers suggest that the polymer does not contain 1,2- and 3,4-microstructure units. From the ^{1}H-NMR spectrum of NBR in Figure 6b, the chemical shift assignments are (CDCl ; δ, ppm), 5.394 (=CH–, 1,4-unit), 4.953 (=CH–, 1,4-unit and =CH_2, 1,2-unit), 2.568 (CHCN, ACN), 2.266 (–CH_2–, 1,4-unit), 2.058 (>CH–, 1,2-unit), 1.639 (–CH_2 , ACN) and 0.820 (–CH_2–, 1,2-unit). Like isoprene, butadiene could undergo polymerization to produce several isomers, which includes the 1,4- and 1,2-addition polymer. From the ^{1}H-NMR spectrum, it showed that the NBR contained both the isomers of polymerized butadiene.

3.2.2. Thermal analysis

DSC thermograms of the rubber films in Figure 7 show that the T_g values of NIR are –9.4 °C for NIR20, 6.2 °C for NIR30, and 20.2 °C for NIR35. T_g of NIR shifted towards higher temperatures with increasing ACN content in the rubber. At high loading of ACN, there are more nitrile groups in the rubber to yield stronger dipolar interaction, which could restrict the movement of rubber chains, and consequently increases the T_g of the rubber film. Because of the strong dipolar interaction between the nitrile groups, pure poly(acrylonitrile) is a brittle plastic with T_g around 85–110 °C, and acrylonitrile is regarded as a hard monomer. Linear poly(isoprene) with high 1,4-units, on the other hand, reported T_g of about –70 °C [19, 30, 31]. Considering that NIR is produced from the copolymerization of both the soft and hard monomers, it is reasonable to expect the T_g of the resultant NIR rubber to lie between those of poly(acrylonitrile) and poly(isoprene). Typical T_g of NBR was reported to be from –38 °C in 18% ACN content up to –2 °C in 50% ACN content [32, 33]. Overall, the T_g of NIR in this work lies within the expected region, albeit slightly higher than that of NBR. More importantly, the T_g of the rubbers, especially NIR20 and NIR30 are well below room temperature, enabling them to remain rubbery at ambient operating temperature, while NIR35, which recorded relatively high T_g, behaved more like plastic.

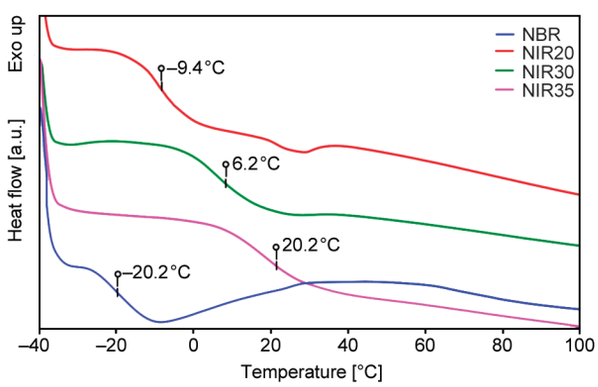

Figure 7. DSC curves of NIR and NBR.

TGA was used to determine the decomposition behavior and thermal stability of the rubber. TGA and DTG curves of all samples are shown in Figure 8. The temperature at 10% weight loss (T_{90}) was used to compare the thermal stability of the rubber samples, and the temperatures recorded for NIR20, NIR30, and NIR35 were 361.3, 366.2, 369.9 °C, respectively. The thermal stability of NIR increased with increasing ACN content, and the same trend was reported by Lee and Ha [34] on the effect of ACN content on the thermal stability of NBR. The increase in thermal stability of the NBR was attributed to the higher decomposition temperature of the nitrile unit compared to the butadiene. This could be the result of the higher energy required to break the strong dipolar interaction contributed by the nitrile group

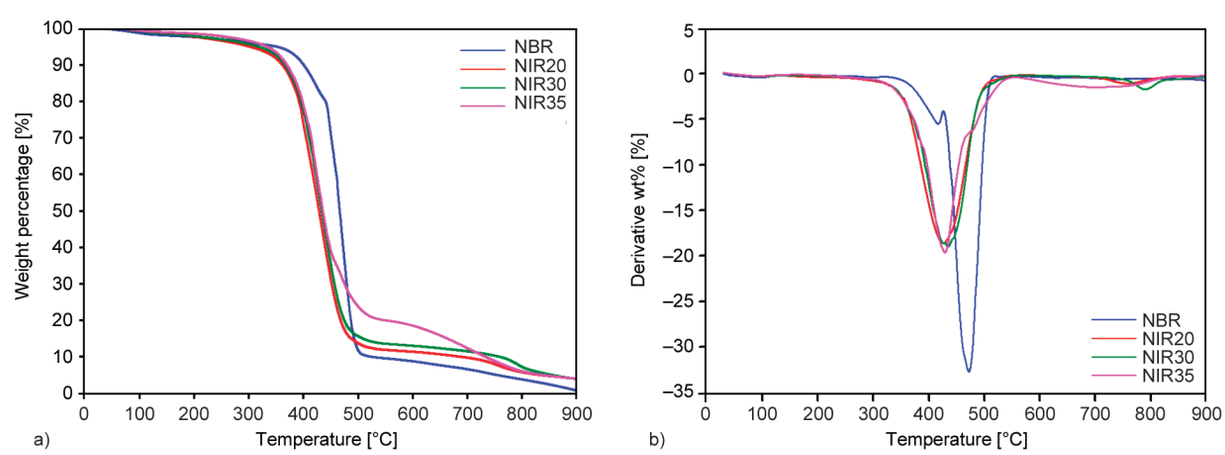

Figure 8. a) TGA curves and b) DTG curves of NIR and NBR.

Table 5. Comparison between decomposition temperature of various NIR and NBR resulted from this work to the recently reported values of NBR in the literature.

Description of sample	ACN content [%]	Decomposition temperatures [°C]			References
		T_{onset}	T_{max}	T_{90}	
NIR20	20*	376.4	426.1	361.3	
NIR30	30*	383.0	434.3	366.2	
NIR35	35*	385.4	428.7	369.9	
NBR	–	430.9	472.0	400.3	
Unfilled NBR	34	–	–	396.6	[35]
+ waste ceramic dust filler		–	–	344.3–381.8	
In situ zirconia filler	34	409.4–414.4	455.4–458.2	–	[36]
Silane-treated silica filler	34	265	445	–	[37]
Unfilled NBR	34	260	418	–	[38]
+ *In situ* silica filler		258–267	437	–	
Nano ZnO filler + disulfochloride benzene crosslinker	40	288	–	350	[39]
Sulfur nd carbon black filler	18	–	449.8	–	[34]
	28	–	453.4	–	
	34	–	456.4	–	
Silica sand nanoparticle filler	40	–	446–456	270–317	[40]
Fumed silica filler		–	450–467	264–286	
Rice bran carbon filler	34	–	461.5–479.9	–	[41]

*based on synthesis formulation

compared to the weak non-polar diene counterpart, resulting in a delay in the overall decomposition of the rubber [34]. Some of the recent reports on decomposition temperatures of NBR are summarized in Table 5, with the value varying from each other due to the differences in the composition of the rubber and its composites. In general, the reported maximum decomposition temperature (T_{max}) of NBR was within a relatively narrow range (418 to 480 °C), while the range of onset decomposition temperature (T_{onset}) and T_{90} varied greatly at 258– 414 °C and 264–396 °C, respectively. Although the thermal stability of NIR is slightly lower compared to the NBR (control) in this study, they are still well within the reported range in the literature and sufficiently high to be used for most elastomeric applications.

3.2.3. Mechanical properties of rubber films

Mechanical property is one important consideration when selecting rubber for a particular application. The mechanical properties of rubber films produced in this work were evaluated according to ASTM D412 for tensile properties and ASTM D624 for tear strength. Stress-strain curves comparison and key mechanical properties are shown in Figure 9 and Table 6, respectively. The *TS* and *EB* follow a similar trend reported in NBR [35, 42], where *TS* increased while *EB* decreased with increasing ACN content. This is attributed to the high strength of dipole interaction between nitrile groups to strengthen the rubber and, at the same time, restrict the rubber chain movement. NIR35 has very low *EB*, exhibiting the behavior of a typical plastic material with necking, as shown in its stress-strain curve. On the other hand, NIR20, NIR30, and NBR films exhibit typical elastomeric

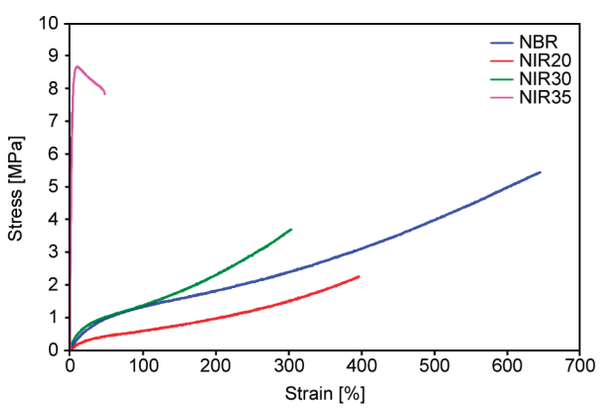

Figure 9. Stress-strain curves of NIR and NBR.

Table 6. Mechanical properties of rubber films.

Sample	*TS* [MPa]	*EB* [%]	*M100* [MPa]	T_s [kN/m]
NIR20	1.61	321	0.585	3.68
NIR30	2.83	253	1.302	7.10
NIR35	8.23	40	n/a	30.53
NBR	6.69	672	1.438	11.03

stress-strain curves. The *TS* and *EB* of NIR20 and NIR30 are, however, lower than that of NBR control films used in this study. This is possibly due to the loss of some unsaturation in the NIR rubber through the formation of crosslinking during the high-temperature emulsion polymerization, which subsequently reduces the effectiveness of the vulcanization process [18]. Although the obtained results for NIR rubber films were lower than the control, the mechanical properties of NIR30 fall well within the reported values for NBR in literature, with *TS* lying between 1.39–9.50 MPa, and *EB* between 227 to 761%, suggesting the viability of NIR to be used for many elastomeric applications [43–46]. *M100* was used to evaluate the stiffness of rubber, and the value increased in the order of NIR20 < NIR30 < NBR. This implies the low rigidity of NIR20 and NIR30 compared to NBR, which could also be attributed to the less effective vulcanization mentioned above. On the other hand, the results of *M100* indicated that *M100* increased as ACN content increased. *M100* for NIR30 is higher than NIR20. The material stiffness enhanced upon ACN content increase, resulting in an increase in modulus. At the same time, it also led to a decrease in *EB* and the *M100* of NIR35 was not measured as the *EB* was <100%. The reported *M100* value of NBR in literature lies between 0.40 to 4.80 MPa [47, 48]. Tear strength, T_s, is defined as the maximum force required to tear the test specimen per unit thickness. The T_s increase with the ACN content in NIR rubber, a trend which was also observed in NBR [42]. Similar to *TS*, the rubber was strengthened by the increased strength of dipole interactions of nitrile groups, improving the resistance of rubber to tearing force. Considering the *TS* values of the rubbers in this work, it was not surprising that NBR has higher T_s than NIR20 and NIR30.

3.2.4. Oil resistance of rubber film

Figure 10a shows the swelling percentage of the rubber film samples in mineral-based engine oil. The oil resistance of the rubber films was evaluated through the percentage of swelling of the films in the hydrocarbon oil. Higher swelling is equivalent to lower oil resistance as the large weight change of the rubber samples indicates higher penetration of oil into the rubber and reduces the entanglement between the rubber chains. Further immersion of rubber samples in oils will cause the formation of pits and cracks through chain scission from thermo-oxidative degradation at elevated temperatures, an environment that is common for oil sealing applications in the automotive industry [49]. These deformations could eventually lead to deterioration in the mechanical properties of the rubber. Hence, an oil resistance test was carried out at room temperature (26 °C) and elevated temperatures of 70 and 100 °C to mimic the usage conditions of oil sealing rubber in the automotive sector. The least oil-resistant synthetic rubber in this work was NBR, with the maximum swelling of 5.46% at 100 °C. For NIR rubber samples, the highest swelling is observed in NIR20, followed by NIR30 and NIR35. Thus, the oil resistance increases in the order from NIR20 < NIR30 < NIR35. The increase in ACN content increases the polarity of NIR rubber, enabling it to repel the penetration of non-polar oil molecules into the rubber matrix through the strong dipolar interaction between nitrile groups. The same phenomenon is also reported in other rubber or blends that exhibit improved oil resistance with increasing polarity, such as in chlorinated NBR [50], NR/dichlorocarbene modified SBR blend [51], and NR/chloroprene blend [52]. The swelling of NBR increases with the testing temperature, which agrees with the reported trend of oil resistance resulting in most rubbers [53, 54]. On the contrary, this trend was not obvious in NIR, possibly due to the minimal swelling of less than 2% in the whole NIR range. The dimension change of NBR rubber at different testing temperatures is shown in Figure 10b. Although the effect and trend from increasing oil temperature on the dimensional changes of the rubber were not that pronounced, possibly because it involves small changes only (<3%), NBR films at 100 °C experienced notably higher dimensional increase than the rest. On the other hand, there was no measurable change in the dimension of all NIR films, and this agrees with the minimal weight changes of the rubber reported in Figure 10a. The NIR and NBR have excellent oil resistance; hence the appearance of NIR20 and NBR did not change noticeably during the oil resistance test as shown in Figures 10c to 10e. NR film was included as a positive control to reflect the superior oil resistance of both synthetic rubbers (NBR and NIR) and validate the experimental protocol. From the comparison in Figures 10c to 10e, it is obvious that NR is the only sample that experienced significant dimensional change post-immersion in mineral oil. Furthermore, the NR sample recorded percentage swelling of 111 and 156% in the

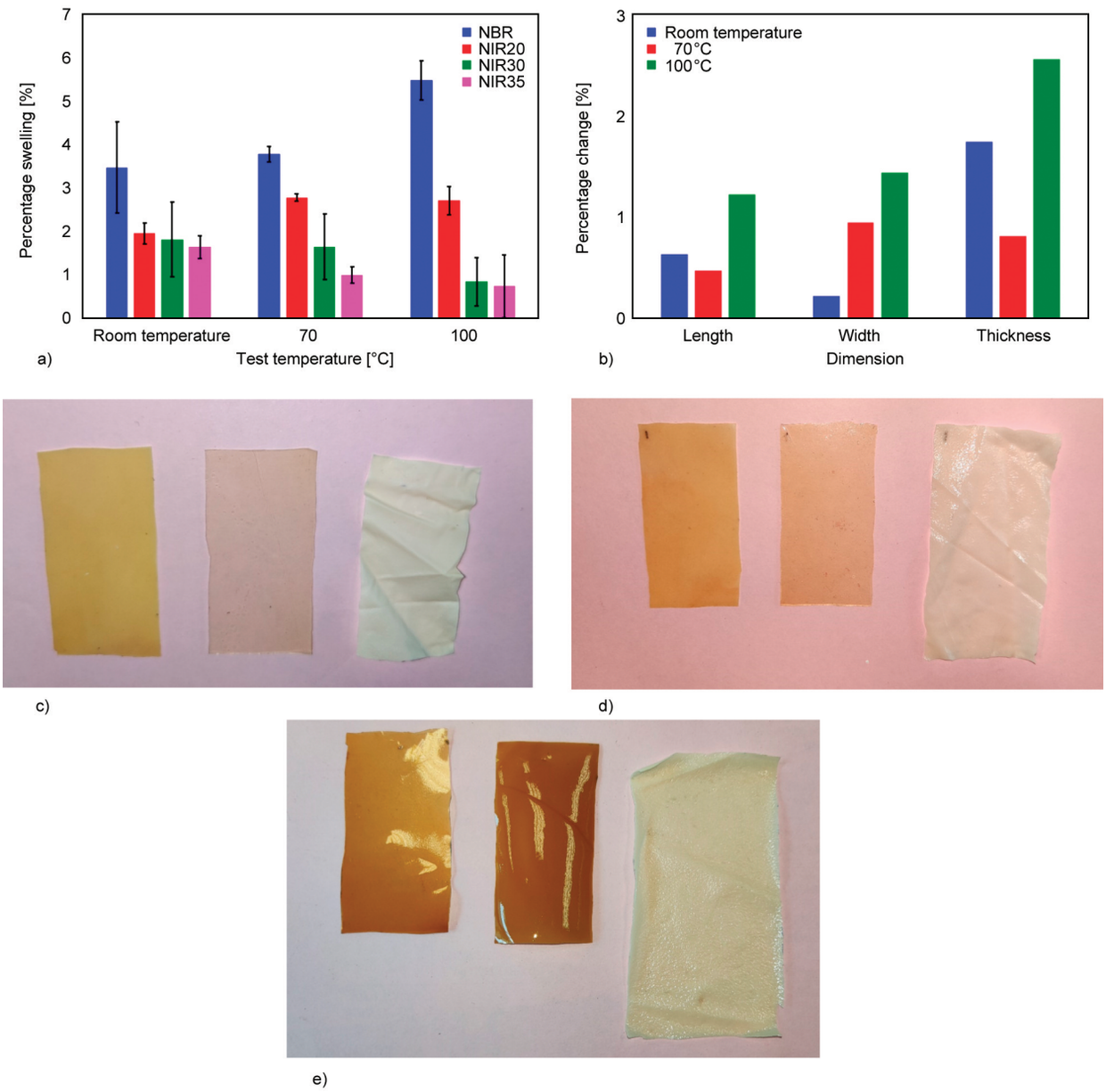

Figure 10. Oil resistance of NIR and NBR films, a) oil swelling, b) dimension change of NBR, and physical appearance of rubber films c) before, and after oil resistance test at d) room temperature and e) 100 °C (from left to right: NIR20, NBR and NR).

oil at room temperature and at 100 °C, respectively, indicating the poor oil resistance of NR compared to NBR and NIR [3]. NIR30 and NIR35 exhibited the best oil resistance with swelling of less than 2% at all testing temperatures. Considering that NIR30 has adequate mechanical properties with superior oil resistance, the rubber may potentially serve as an alternative to NBR in applications that requires good oil resistance, such as joint seals and automotive parts.

4. Conclusions

In this work, a series of poly(isoprene-*co*-acrylonitrile), NIR rubbers with varying ACN content were synthesized via free radical emulsion polymerization. NIR rubber emulsions have good stability, evidenced by the small particle size of the emulsion in the range 90.7 to 122.0 nm, monodisperse (polydispersity indices <0.07), and high magnitude of zeta potential, –63.3 to –50.1 mV. The chemical structure of the synthesized rubber was characterized using FTIR and ^{1}H-NMR, and the results indicated that the polymerization was successful, and the polymerized isoprene in the rubber was predominantly of 1,4-microstructure. The vulcanized NIR films displayed glass transition temperatures from –9.4 to 20.2 °C, of which NIR20 and NIR30 exhibit rubbery behavior

at ambient temperature while NIR35 behaved more towards plastic. The synthesized rubber also recorded good thermal stability, comparable to the control nitrile rubber used in this study. As for mechanical property, ultimate tensile strength and tear strength of the NIR rubbers increased, but elongation at break decreased with ACN content, and although the values are within the reported range in literature, it falls short compared to the NBR control used in this study. On the contrary, the oil resistance of NIR rubber films is superior to the NBR control. In conclusion, NIR has decent thermal stability, mechanical strength, and excellent oil resistance and could serve as an alternative to NBR which had been traditionally used for oil resistance applications. Using isoprene in NIR formulation instead of butadiene gas in NBR formulation could be advantageous in terms of ease of production setup and lower hazard risk.

Acknowledgements

We would like to acknowledge the financial support from the Ministry of Higher Education Malaysia through the Fundamental Research Grant Scheme, FRGS, Project number FRGS/1/2021/STG04/UM/02/4.

References

[1] Gent A. N.: Rubber elasticity: Basic concepts and behavior. in 'The science and technology of rubber' (eds.: Erman B., Mark J. E., Roland C. M.) Elsevier, Waltham, 1–26 (2022). https://doi.org/10.1016/B978-0-12-394584-6.00001-7

[2] Arias M., van Dijk P. J.: What is natural rubber and why are we searching for new sources? Frontiers for Young Minds, **7**, 100 (2019). https://doi.org/10.3389/frym.2019.00100

[3] Simpson R. B.: Rubber basics. Rapra Technology, Shrewsbury (2007).

[4] Boon Z. H., Teo Y. Y., Ang D. T-C.: Recent development of biodegradable synthetic rubbers and bio-based rubbers using sustainable materials from biological sources. RSC Advances, **12**, 34028–34052 (2022). https://doi.org/10.1039/D2RA06602E

[5] Sarkar P., Bhowmick A. K.: Sustainable rubbers and rubber additives. Journal of Applied Polymer Science, **135**, 45701 (2018). https://doi.org/10.1002/app.45701

[6] Fukahori Y.: Use of natural rubber (NR) for vibration isolation and earthquake protection of structures. in 'Chemistry, manufacture and applications of natural rubber' (eds.: Nakao T., Kohjiya S.) Elsevier, Cambridge 371–381 (2014). https://doi.org/10.1533/9780857096913.2.371

[7] Toki S.: The effect of strain-induced crystallization (SIC) on the physical properties of natural rubber (NR). in 'Chemistry, manufacture and applications of natural rubber' (eds.: Nakao T., Kohjiya S.) Elsevier, Cambridge, 135–167 (2014). https://doi.org/10.1533/9780857096913.1.135

[8] Zheng T., Zheng X., Zhan S., Zhou J., Liao S.: Study on the ozone aging mechanism of natural rubber. Polymer Degradation and Stability, **186**, 109514 (2021). https://doi.org/10.1016/j.polymdegradstab.2021.109514

[9] Ali M. F., Akber M. A., Smith C., Aziz A. A.: The dynamics of rubber production in Malaysia: Potential impacts, challenges and proposed interventions. Forest Policy and Economics, **127**, 102449 (2021). https://doi.org/10.1016/j.forpol.2021.102449

[10] Linhares F. N., Corrêa H. L., Khalil C. N., Amorim Moreira Leite M. C., Guimarães Furtado C. R.: Study of the compatibility of nitrile rubber with Brazilian biodiesel. Energy, **49**, 102–106 (2013). https://doi.org/10.1016/j.energy.2012.10.040

[11] Sisanth K. S., Thomas M. G., Abraham J., Thomas S.: General introduction to rubber compounding. in 'Progress in rubber nanocomposites' (eds.: Thomas S., Maria H. J.) Elsevier, Duxford, 1–39 (2017). https://doi.org/10.1016/B978-0-08-100409-8.00001-2

[12] Franta I.: Elastomers and rubber compounding materials: Manufacture, properties and applications. Elsevier, New York (1989).

[13] Jones M. D.: Catalytic transformation of ethanol into 1,3-butadiene. Chemistry Central Journal, 8, 53 (2014). https://doi.org/10.1186/s13065-014-0053-4

[14] Quirk R. P., Pickel D. L.: Polymerization: Elastomer synthesis. in 'The science and technology of rubber' (eds.: Erman B., Mark J. E., Roland C. M.) Elsevier, Waltham, 27–113 (2022). https://doi.org/10.1016/B978-0-12-394584-6.00002-9

[15] Hsieh H. L.: Kinetics of polymerization of butadiene, isoprene, and styrene with alkyllithiums. Part II. Rate of initiation. Journal of Polymer Science Part A: General Papers, **3**, 163–172 (1965). https://doi.org/10.1002/pol.1965.100030118

[16] Weerts P. A., Loos J. L. M., German A. L.: Initiation phenomena in the emulsion polymerization of butadiene and isoprene. Polymer Communications, **29**, 278–279 (1988).

[17] Apolinar Y., Ramos L. F., Saade H., Díaz de León R., López R. G.: Polyisoprene nanoparticles prepared by polymerization in microemulsion. Journal of Nanomaterials, **2010**, 549264 (2010). https://doi.org/10.1155/2010/549264

[18] Cheong I. W., Fellows C. M., Gilbert R. G.: Synthesis and cross-linking of polyisoprene latexes. Polymer, **45**, 769–781 (2004). https://doi.org/10.1016/j.polymer.2003.12.002

[19] Chouytan J., Beraheng S., Kalkornsurapranee E., Fellows C. M., Kaewsakul W.: Synthesis of polyisoprene *via* miniemulsion polymerisation: Effect on thermal behaviour, colloidal properties and stereochemistry. Journal of Rubber Research, **21**, 236–255 (2018). https://doi.org/10.1007/BF03449173

[20] Lima R., de Santi D.: Process for the preparation of nitrile rubbers. European Patent EP 2723776 B1, EU (2013).

[21] Tsuji S., Uchizono Y.: Unsaturated nitrile-conjugated diene copolymer, process for producing same and vulcanizable rubber composition. US5703189A, United States (1997).

[22] Rahn-Chique K., Urbina-Villalba G.: Dependence of emulsion stability on particle size: Relative importance of drop concentration and destabilization rate on the half lifetimes of O/W nanoemulsions. Journal of Dispersion Science and Technology, **38**, 167–179 (2017). https://doi.org/10.1080/01932691.2016.1149715

[23] Corcorran S., Lochhead R. Y., McKay T.: Particle-stabilized emulsions: A brief overview. Cosmetics and Toiletries, **119**, 47–52 (2004).

[24] Danaei M., Dehghankhold M., Ataei S., Hasanzadeh Davarani F., Javanmard R., Dokhani A., Khorasani S., Mozafari M.: Impact of particle size and polydispersity index on the clinical applications of lipidic nanocarrier systems. Pharmaceutics, **10**, 57 (2018). https://doi.org/10.3390/pharmaceutics10020057

[25] Joseph E., Singhvi G.: Multifunctional nanocrystals for cancer therapy: A potential nanocarrier. in 'Nanomaterials for drug delivery and therapy' (eds.: Grumezescu A. M.) Elsevier, Oxford, 91–116 (2019). https://doi.org/10.1016/B978-0-12-816505-8.00007-2

[26] Gumustas M., Sengel-Turk C. T., Gumustas A., Ozkan S. A., Uslu B.: Effect of polymer-based nanoparticles on the assay of antimicrobial drug delivery systems. in 'Multifunctional systems for combined delivery, biosensing and diagnostics' (eds.: Grumezescu A. M.) Elsevier, Oxford, 67–108 (2017). https://doi.org/10.1016/B978-0-323-52725-5.00005-8

[27] Daik R., Bidol S., Abdullah I.: Effect of molecular weight on the droplet size and rheological properties of liquid natural rubber emulsion. Malaysian Polymer Journal, **2**, 29–38 (2007).

[28] He A., Wang G., Zhao W., Jiang X., Yao W., Sun W-H.: High *cis*-1,4 polyisoprene or *cis*-1,4/3,4 binary polyisoprene synthesized using 2-(benzimidazolyl)-6-(1-(arylimino)ethyl)pyridine cobalt(II) dichlorides. Polymer International, **62**, 1758–1766 (2013). https://doi.org/10.1002/pi.4490

[29] Chen D., Shao H., Yao W., Huang B.: Fourier transform infrared spectral analysis of polyisoprene of a different microstructure. International Journal of Polymer Science, **2013**, 937284 (2013). https://doi.org/10.1155/2013/937284

[30] Howard W. H.: The glass temperatures of polyacrylonitrile and acrylonitrile–vinyl acetate copolymers. Journal of Applied Polymer Science, **5**, 303–307 (1961). https://doi.org/10.1002/app.1961.070051509

[31] Kow C., Morton M., Fetters L. J., Hadjichristidis N.: Glass transition behavior of polyisoprene: The influence of molecular weight, terminal hydroxy groups, microstructure, and chain branching. Rubber Chemistry and Technology, **55**, 245–252 (1982). https://doi.org/10.5254/1.3535872

[32] Makhiyanov N., Temnikova E. V.: Glass-transition temperature and microstructure of polybutadienes. Polymer Science Series A, **52**, 1292–1300 (2010). https://doi.org/10.1134/S0965545X10120072

[33] Ambler M. R.: Studies on the nature of multiple glass transitions in low acrylonitrile, butadiene–acrylonitrile rubbers. Journal of Polymer Science: Polymer Chemistry Edition, **11**, 1505–1515 (1973). https://doi.org/10.1002/pol.1973.170110704

[34] Lee Y. S., Ha K.: Effects of acrylonitrile content on thermal characteristics and thermal aging properties of carbon black-filled NBR composite. Journal of Elastomers and Plastics, **53**, 402–416 (2021). https://doi.org/10.1177/0095244320941243

[35] El-Nemr K. F., El-Naggar M. Y., Fathy E. S.: Waste ceramic dust activated by gamma radiation and coupling agents as reinforcement for nitrile rubber. Journal of Vinyl and Additive Technology, **24**, 37–43 (2018). https://doi.org/10.1002/vnl.21515

[36] Ambilkar S. C., Bansod N. D., Kapgate B. P., Das A., Formanek P., Rajkumar K., Das C.: *In situ* zirconia: A superior reinforcing filler for high-performance nitrile rubber composites. ACS Omega, **5**, 7751–7761 (2020). https://doi.org/10.1021/acsomega.9b03495

[37] Kapgate B. P., Das C., Basu D., Das A., Heinrich G.: Rubber composites based on silane-treated stöber silica and nitrile rubber. Journal of Elastomers and Plastics, **47**, 248–261 (2015). https://doi.org/10.1177/0095244313507807

[38] Kapgate B. P., Das C., Basu D., Das A., Heinrich G., Reuter U.: Effect of silane integrated sol-gel derived *in situ* silica on the properties of nitrile rubber. Journal of Applied Polymer Science, **131**, 40531 (2014). https://doi.org/10.1002/app.40531

[39] Mammadov S. M., Khankishiyeva R. F., Ramazanov M. A., Akbarov O. H., Akhundzada H. N.: Influence of gamma irradiation on structure and properties of nitrile-butadien rubber in presence of modified nano metals. American Journal of Polymer Science, **7**, 23–29 (2017). https://doi.org/10.5923/j.ajps.20170702.01

[40] Eyssa H. M., Abulyazied D. E., Abdulrahman M., Youssef H. A.: Mechanical and physical properties of nanosilica/nitrile butadiene rubber composites cured by gamma irradiation. Egyptian Journal of Petroleum, **27**, 383–392 (2018). https://doi.org/10.1016/j.ejpe.2017.06.004

[41] Li M-C., Zhang Y., Cho U. R.: Mechanical, thermal and friction properties of rice bran carbon/nitrile rubber composites: Influence of particle size and loading. Materials and Design, **63**, 565–574 (2014). https://doi.org/10.1016/j.matdes.2014.06.032

[42] Yasin T., Ahmed S., Yoshii F., Makuuchi K.: Effect of acrylonitrile content on physical properties of electron beam irradiated acrylonitrile–butadiene rubber. Reactive and Functional Polymers, **57**, 113–118 (2003). https://doi.org/10.1016/j.reactfunctpolym.2003.08.004

[43] Ruan M., Yang D., Guo W., Zhang L., Li S., Shang Y., Wu Y., Zhang M., Wang H.: Improved dielectric properties, mechanical properties, and thermal conductivity properties of polymer composites via controlling interfacial compatibility with bio-inspired method. Applied Surface Science, **439**, 186–195 (2018). https://doi.org/10.1016/j.apsusc.2017.12.250

[44] Bova T., Tran C. D., Balakshin M. Y., Chen J., Capanema E. A., Naskar A. K.: An approach towards tailoring interfacial structures and properties of multiphase renewable thermoplastics from lignin–nitrile rubber. Green Chemistry, **18**, 5423–5437 (2016). https://doi.org/10.1039/C6GC01067A

[45] Marzec A., Laskowska A., Boiteux G., Zaborski M., Gain O., Serghei A.: The impact of imidazolium ionic liquids on the properties of nitrile rubber composites. European Polymer Journal, **53**, 139–146 (2014). https://doi.org/10.1016/j.eurpolymj.2014.01.035

[46] Szadkowski B., Marzec A., Rybiński P.: Silane treatment as an effective way of improving the reinforcing activity of carbon nanofibers in nitrile rubber composites. Materials, **13**, 3481 (2020). https://doi.org/10.3390/ma13163481

[47] Gill Y. Q., Irfan M. S., Saeed F., Nadeem M., Ehsan H.: Silanized silica compatibilization of NBR/gelatin blends for the production of green rubber products. Journal of Elastomers and Plastics, **51**, 457–472 (2019). https://doi.org/10.1177/0095244318798142

[48] Senthivel K., Manikandan K., Prabu B.: Studies on the mechanical properties of carbon black/halloysite nanotube hybrid fillers in nitrile rubber nanocomposites. Materials Today: Proceedings, **2**, 3627–3637 (2015). https://doi.org/10.1016/j.matpr.2015.07.118

[49] Lou W., Zhang W., Wang H., Jin T., Liu X.: Influence of hydraulic oil on degradation behavior of nitrile rubber O-rings at elevated temperature. Engineering Failure Analysis, **92**, 1–11 (2018). https://doi.org/10.1016/j.engfailanal.2018.05.006

[50] Nihmath A., Ramesan M. T.: Synthesis, characterization, processability, mechanical properties, flame retardant, and oil resistance of chlorinated acrylonitrile butadiene rubber. Polymers for Advanced Technologies, **29**, 2165–2173 (2018). https://doi.org/10.1002/pat.4324

[51] Ramesan M. T., Alex R., Khanh N. V.: Studies on the cure and mechanical properties of blends of natural rubber with dichlorocarbene modified styrene–butadiene rubber and chloroprene rubber. Reactive and Functional Polymers, **62**, 41–50 (2005). https://doi.org/10.1016/j.reactfunctpolym.2004.08.002

[52] Tanrattanakul V., Wattanathai B., Tiangjunya A., Muhamud P.: *In situ* epoxidized natural rubber: Improved oil resistance of natural rubber. Journal of Applied Polymer Science, **90**, 261–269 (2003). https://doi.org/10.1002/app.12706

[53] Zielińska M., Seyger R., Dierkes W. K., Bielinski D., Noordermeer J. W.: Swelling of EPDM rubbers for oil-well applications as influenced by medium composition and temperature. Part I. Literature and theoretical background. Elastomery, **20**, 6–17 (2016).

[54] Lou W., Zhang W., Jin T., Liu X., Dai W.: Synergistic effects of multiple environmental factors on degradation of hydrogenated nitrile rubber seals. Polymers, **10**, 897 (2018). https://doi.org/10.3390/polym10080897